Constant Boost Control of the Z-Source Inverter to Minimize Current Ripple and Voltage Stress

Miaosen Shen, *Student Member, IEEE*, Jin Wang, *Member, IEEE*, Alan Joseph, Fang Zheng Peng, *Fellow, IEEE*, Leon M. Tolbert, *Senior Member, IEEE*, and Donald J. Adams, *Member, IEEE*

***Abstract*—This paper proposes two constant boost-control methods for the Z-source inverter, which can obtain maximum voltage gain at any given modulation index without producing any low-frequency ripple that is related to the output frequency and minimize the voltage stress at the same time. Thus, the Z-network requirement will be independent of the output frequency and determined only by the switching frequency. The relationship of voltage gain to modulation index is analyzed in detail and verified by simulation and experiments.**

***Index Terms*—Pulsewidth modulation (PWM), voltage boost, Z-source inverter.**

I. Introduction

In A traditional voltage-source inverter, the two switches of the same-phase leg can never be gated on at the same time because doing so would cause a short circuit (shoot through) to occur, which would destroy the inverter. In addition, the maximum output voltage obtainable can never exceed the dc bus voltage. These limitations can be overcome by the new Z-source inverter [1], shown in Fig. 1, which uses an impedance network (Z network) to replace the traditional dc link. The Z-source inverter advantageously utilizes the shoot-through states to boost the dc-bus voltage by gating on both the upper and lower switches of a phase leg. Therefore, the Z-source inverter can buck and boost voltage to a desired output voltage that is greater than the available dc bus voltage. In addition, the reliability of the inverter is greatly improved because the shoot through caused by electromagnetic interference (EMI) noise can no longer destroy the circuit. Thus, it provides a low-cost, reliable, and highly efficient single-stage structure for buck and boost power conversion.

Paper IPCSD-06-005, presented at the 2004 Industry Applications Society Annual Meeting, Seattle, WA, October 3–7, and approved for publication in the IEEE TRANSACTIONS ON INDUSTRY APPLICATIONS by the Industrial Power Converter Committee of the IEEE Industry Applications Society. Manuscript submitted for review October 15, 2004 and released for publication February 10, 2006. This work was supported in part by the DoE FreedomCar Program via Oak Ridge National Laboratory and in part by the National Science Foundation under Grant 0424039.

M. Shen, A. Joseph, and F. Z. Peng are with the Department of Electrical and Computer Engineering, Michigan State University, East Lansing, MI 48824 USA (e-mail: shenmiao@msu.edu; josepha2@egr.msu.edu; fzpeng@egr.msu.edu).

J. Wang is with Ford Motor Company, Dearborn, MI 48120-1261 USA (e-mail: jwang78@ford.com).

L. M. Tolbert is with the University of Tennessee, Knoxville, TN 37996-2100 USA (e-mail: tolbert@utk.edu).

D. J. Adams is with National Transportation Research Center, Oak Ridge National Laboratory, Knoxville, TN 37932 USA (e-mail: adamsdj@ornl.gov).

Digital Object Identifier 10.1109/TIA.2006.872927

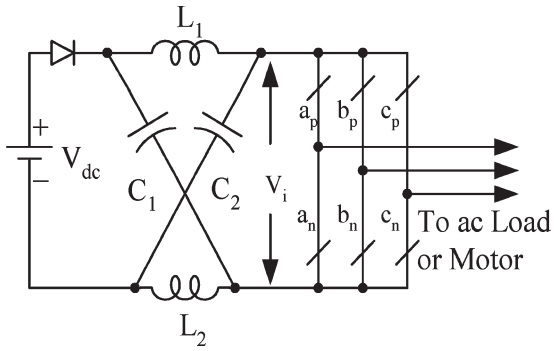

Fig. 1. Z-source inverter.

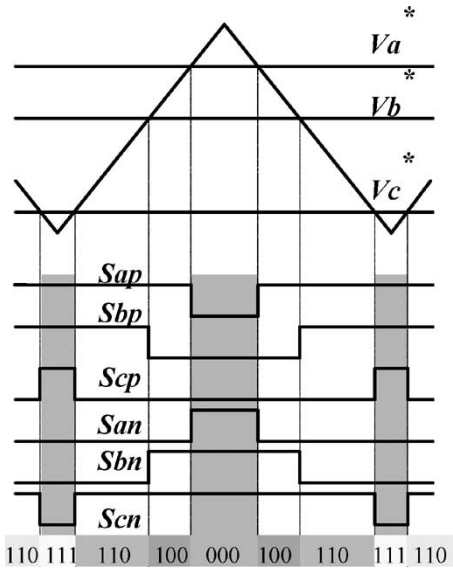

Fig. 2. Carrier-based PWM for traditional voltage-source inverter.

Pulsewidth-modulation (PWM) control for the Z-source inverter has to be modified to utilize the shoot-through states for voltage boost. Fig. 2 shows the traditional carrier-based PWM scheme of the voltage-source inverter. There are eight permissible switching states: six active and two zero states. During the two zero states, the upper three or the lower three switches are turned on simultaneously, thus shorting the output terminals of the inverter and producing zero voltage to the load. During one of the six active states, the dc voltage is impressed across the load, positively or negatively. In addition to the eight traditional switching states, the Z-source inverter has several shoot-through zero states, during which both the upper and lower switches of one or multiple same-phase legs

are turned on. It is obvious that during a shoot-through zero state, the output terminals of the inverter are shorted and the output voltage to the load is zero. Therefore, the shoot-through states have the same effect (i.e., zero voltage) to the load as the traditional zero states; however, these shoot-through states can boost the dc voltage. The active states have to be kept unchanged to maintain the output voltage waveform, and the traditional zero states can be replaced partially or entirely by the shoot-through zero states depending on how much voltage boost is needed.

Several modified PWM control methods for the Z-source inverter based on traditional control methods were presented in [7]. A simple control method was introduced in [1], which uses two straight lines to control the shoot-through states. A maximum boost control was presented in [2]. The proposed method in [2] can achieve the minimum voltage stress across the switches. However, it has the drawbacks of low-frequency ripples on the Z-source network, which will be discussed in detail in Section II. In this paper, we will present two control methods to achieve maximum voltage boost/gain while maintaining a constant boost viewed from the Z-source network and producing no low-frequency ripples associated with the output frequency. This maximum constant boost control can greatly reduce the L and C requirements of the Z-network. The relationship of voltage boost and modulation index, as well as the voltage stress on the devices, will be investigated and verified by simulation and experiments.

II. Voltage Boost, Stress, and Current Ripple

As described in [1], the voltage gain G of the Z-source inverter can be expressed as

$$G = \frac{\hat{V}_{\rm o}}{V_{\rm dc}/2} = MB \tag{1}$$

and

$$B = \frac{1}{1 - 2\frac{T_0}{T}} \tag{2}$$

where $\hat{V}_{\rm o}$ is the peak value of the output phase voltage, $V_{\rm dc}$ is the input dc voltage, M is the modulation index, and B is the boost factor determined by the shoot-through time interval (T_0) over a switching cycle (T), or the shoot-through duty ratio $(T_0/T = D_0)$.

In [1], a simple boost-control method was used to control the shoot-through duty ratio. In this case, the shoot-through time per switching cycle is kept constant, thus having a constant boost factor. As a result, the dc inductor current and capacitor voltage have no ripples that are associated with the output frequency. As shown in [2], this simple boost control's obtainable shoot-through duty ratio decreases with the increase of M, and the resulting voltage stress across the devices is relatively high. To obtain the maximum voltage boost, Peng *et al.* [2] presented the maximum boost-control method, as shown in Fig. 3, which shoots through all zero states entirely. Based on the map in Fig. 3, the shoot-through duty cycle D_0 varies at six times the output frequency. As discussed in [2], the voltage boost

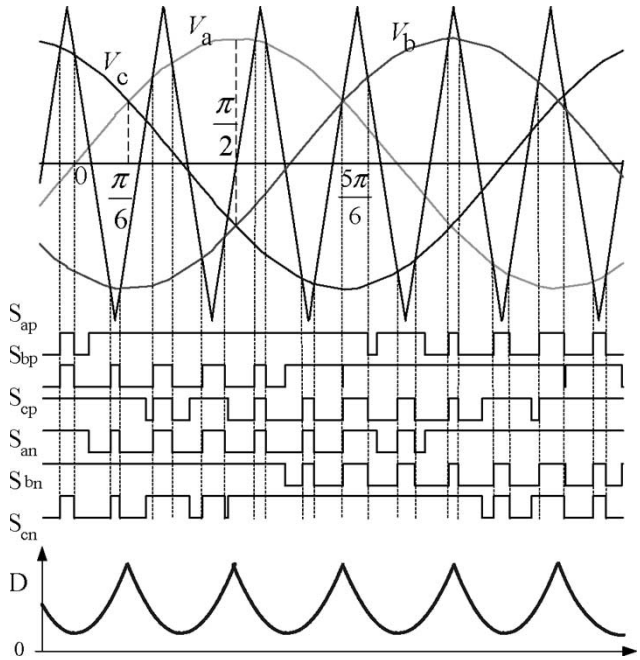

Fig. 3. Maximum boost-control sketch map.

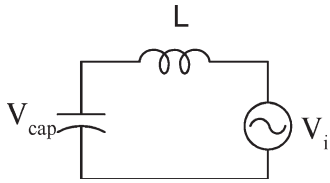

Fig. 4. Model of the circuit.

is inversely related to the shoot-though duty ratio; therefore, the ripple in shoot-through duty ratio will result in ripple in the current through the inductor, as well as in the voltage across the capacitor. When the output frequency is low, the inductor current ripple becomes significant, and a large inductor is required.

To calculate the current ripple through the inductor, the circuit can be modeled as in Fig. 4, where L is the inductor in the Z-source network, $V_{\rm Cap}$ is the voltage across the capacitor in the Z-source network, and $V_{\rm i}$ is the voltage fed to the inverter. Neglecting the switching-frequency element, the average value of $V_{\rm i}$ can be described as

$$\overline{V}_{\rm i} = (1 - D_0)BV_{\rm dc}. \tag{3}$$

From [2], we have

$$D_0(\omega t) = \frac{2 - \left(M\sin\omega t - M\sin\left(\omega t - \frac{2}{3}\pi\right)\right)}{2}$$
$$= 1 - \frac{\sqrt{3}}{2}M\cos\left(\omega t - \frac{1}{3}\pi\right) \quad \left(\frac{\pi}{6} < \omega t < \frac{\pi}{2}\right) \tag{4}$$

where ω is the output angular frequency.

The boost factor is

$$B = \frac{\pi}{3\sqrt{3}M - \pi}. \tag{5}$$

As can be seen from (4), D_0 has the minimum value at $\omega t = (\pi/3)$ and has the maximum value at $\omega t = (\pi/6)$ or $\omega t = (\pi/2)$. Assuming the voltage across the capacitor is constant, the voltage ripple across the inductor $V_{\rm pk2pk}$ can be approximated as a sinusoid with a peak-to-peak value of

$$\begin{aligned} V_{\rm pk2pk} &= V_{\rm i\,max} - V_{\rm i\,min} \\ &= \left(\frac{\sqrt{3}}{2}M - \frac{\sqrt{3}}{2}M\cos\left(\frac{\pi}{6}\right)\right)BV_{\rm dc} \\ &= \frac{\left(\frac{\sqrt{3}}{2} - \frac{3}{4}\right)M\pi}{3\sqrt{3}M - \pi}V_{\rm dc}. \end{aligned} \tag{6}$$

Therefore, the current ripple through the inductor becomes

$$\Delta I_L = \frac{V_{\rm pk2pk}}{6\omega L} = \frac{(2\sqrt{3}-3)M\pi V_{\rm dc}}{24(3\sqrt{3}M - \pi)\omega L} \tag{7}$$

where $L = L_1 = L_2$.

As can be seen from (7), the inductor has to be large for low output frequency in order to limit the current ripple within a certain range.

By turning all zero states into shoot-through states, the Z-source inverter achieves the maximum boost and minimizes the voltage stress. The maximum boost control presented in [2] thus requires the minimum voltage rating for the switching devices at a given available input voltage and desired output voltage. However, this method introduces a low-frequency current ripple that is associated with the output frequency in the inductor current and the capacitor voltage. This will cause a higher requirement of the passive components when the output frequency becomes very low. Therefore, the maximum boost control is suitable for applications that have a fixed or relatively high output frequency and the six-time frequency current ripple is not a problem. For applications with variable and low output frequency, the method may require a large dc inductor.

III. Maximum Constant Boost Control

In order to reduce the volume and cost of the Z-source network, we need to eliminate the low-frequency current ripple by using a constant shoot-through duty ratio. At the same time, a greater voltage boost for any given modulation index is desired to reduce the voltage stress across the switches. Fig. 5 shows the sketch map of the maximum constant boost-control method proposed in this paper, which achieves the maximum voltage gain while always keeping the shoot-through duty ratio constant. There are five modulation curves in this control method: three reference signals $V_{\rm a}$, $V_{\rm b}$, and $V_{\rm c}$, and two shoot-through envelope signals $V_{\rm p}$ and $V_{\rm n}$. When the carrier triangle wave is higher than the upper shoot-through envelope $V_{\rm p}$ or lower than the bottom shoot-through envelope $V_{\rm n}$, the inverter is turned to a shoot-through zero state. In between, the inverter switches in the same way as in the traditional carrier-based PWM control.

Because the boost factor is determined by the shoot-though duty cycle, as expressed in (2), the shoot-through duty cycle must be kept the same from switching cycle to switching cycle in order to maintain a constant boost. The basic point is to get the maximum B while keeping it constant all the time. The upper and lower envelope curves are periodical and are three times the output frequency. There are two half-periods for both curves in a cycle.

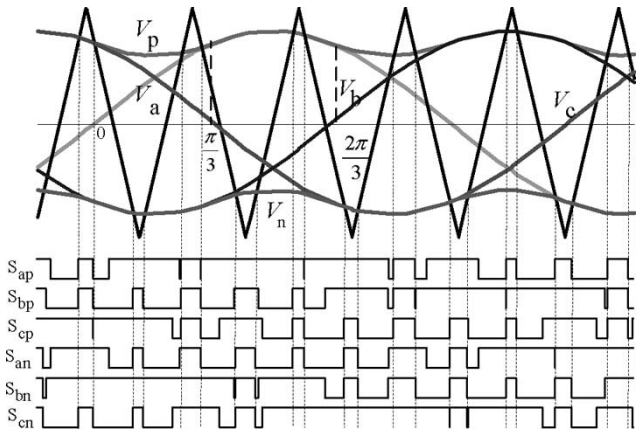

Fig. 5. Sketch map of constant boost control.

For the first half-period, $[0, \pi/3]$ in Fig. 5, the upper and lower envelope curves can be expressed by (8) and (9), respectively

$$V_{\rm p1} = \sqrt{3}M + \sin\left(\theta - \frac{2\pi}{3}\right)M, \qquad \text{for } 0 < \theta < \frac{\pi}{3} \tag{8}$$

$$V_{\rm n1} = \sin\left(\theta - \frac{2\pi}{3}\right)M, \qquad \text{for } 0 < \theta < \frac{\pi}{3}. \tag{9}$$

For the second half-period $[\pi/3, 2\pi/3]$, the envelope curves are expressed by (10) and (11), respectively

$$V_{\rm p2} = \sin(\theta)M, \qquad \text{for } \frac{\pi}{3} < \theta < \frac{2\pi}{3} \tag{10}$$

$$V_{\rm n2} = \sin(\theta)M - \sqrt{3}M, \qquad \text{for } \frac{\pi}{3} < \theta < \frac{2\pi}{3}. \tag{11}$$

Obviously, the distance between these two curves determining the shoot-through duty ratio is always constant for a given modulation index M, that is, $\sqrt{3}M$. Therefore, the shoot-through duty ratio is constant and can be expressed as

$$\frac{T_0}{T} = \frac{2 - \sqrt{3}M}{2} = 1 - \frac{\sqrt{3}M}{2}. \tag{12}$$

The boost factor B and the voltage gain G can be calculated as follows

$$B = \frac{1}{1 - 2\frac{T_0}{T}} = \frac{1}{\sqrt{3}M - 1} \tag{13}$$

$$G = \frac{\hat{V}_{\rm o}}{V_{\rm dc}/2} = MB = \frac{M}{\sqrt{3}M - 1}. \tag{14}$$

The curve of voltage gain versus modulation index is shown in Fig. 6. The voltage gain approaches infinity when M decreases to $\sqrt{3}/3$.

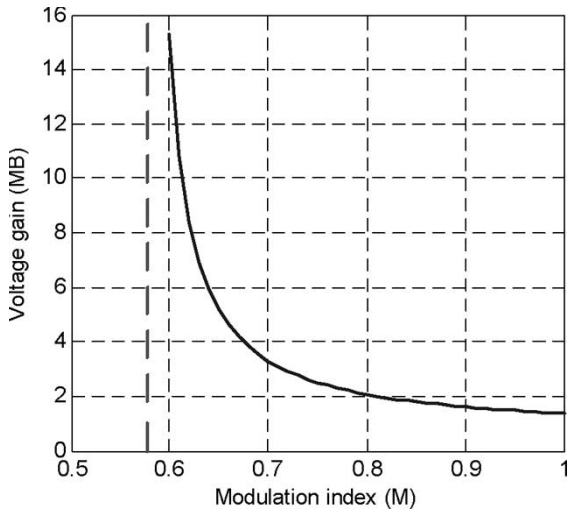

Fig. 6. Voltage gain (MB) versus M.

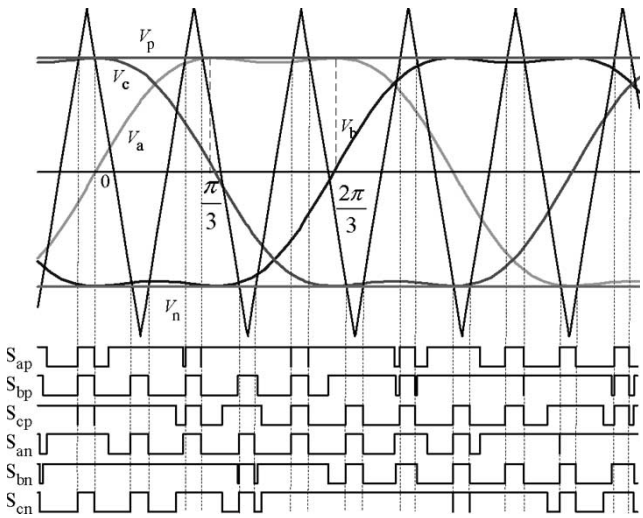

Fig. 7. Sketch map of constant boost control with third-harmonic injection.

From Fig. 5, we can see that the upper shoot-through envelope is always equal to or higher than the maximum value of the reference signals, and the lower shoot-through envelope is always equal to or lower than the minimum value of the reference signals. Therefore, the shoot-though states only occur during the traditional zero states from the traditional carrier-based PWM control. As a result, this control maintains the output waveform.

It can be easily seen from the above analysis that the shoot-through duty ratio is always constant. This can be reconfirmed from a different perspective below. For modulation index M, the maximum active-state duty ratio $D_{\mathrm{a\,max}}$ can be expressed as

$$D_{\mathrm{a\,max}} = \max\left(\frac{M\sin\omega t - M\sin\left(\omega t - \frac{2\pi}{3}\right)}{2}\right) = \frac{\sqrt{3}}{2}M \tag{15}$$

where $D_{\mathrm{a\,max}}$ is the maximum duty ratio of the active states combined in a switching cycle. In order to keep the active states unchanged while making the shoot-through duty ratio always constant, the maximum shoot-through duty ratio that can be achieved is

$$D_{0\,\max} = 1 - D_{\mathrm{a\,max}} = 1 - \frac{\sqrt{3}}{2}M. \tag{16}$$

This is exactly the same as the results shown in (12). To summarize, this control method produces the maximum constant boost while minimizing the voltage stress.

The above-proposed maximum constant boost control (Fig. 5) can be implemented alternatively by using third-harmonic injection [3]. A sketch map of the third-harmonic-injection control method is shown in Fig. 7. A third-harmonic component with 1/6 of the fundamental component is injected to the three phase-voltage references. As shown in Fig. 7, V_{a} reaches its peak value $(\sqrt{3}/2)M$ while V_{b} is at its minimum value $-(\sqrt{3}/2)M$ at $\pi/3$. Therefore, a unique feature can be obtained: only two straight lines, V_{p} and V_{n}, are needed to control the shoot-through time with the 1/6 (16%) third-harmonic injection.

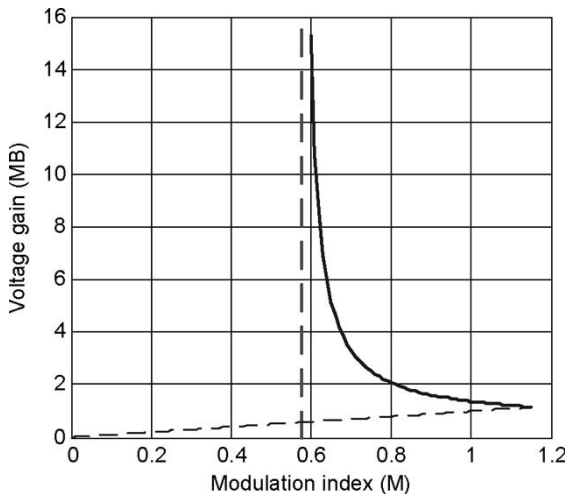

Fig. 8. Voltage gain (MB) versus modulation index (M).

From Fig. 7, the shoot-through duty ratio can be calculated by

$$\frac{T_0}{T} = \frac{2-\sqrt{3}M}{2} = 1 - \frac{\sqrt{3}M}{2} \tag{17}$$

which is identical to the previously proposed maximum constant boost-control method shown in Fig. 5. Therefore, the voltage gain can also be calculated by the same equations (13) and (14). The difference is that the third-harmonic-injection control method has a larger modulation index M, which increased from 1 to $2/\sqrt{3}$. The voltage gain versus M is shown in Fig. 8 for the third-harmonic-injection method. The voltage gain can be varied from infinity to zero smoothly by increasing M from $\sqrt{3}/3$ to $2/\sqrt{3}$ with shoot through, as shown in the solid curve, and then decreasing M from $2/\sqrt{3}$ to zero without shoot through, as shown in the small dashed curve in Fig. 8.

IV. Voltage-Stress Comparison

To examine the voltage stress across the switching devices, an equivalent dc voltage is introduced. The equivalent dc

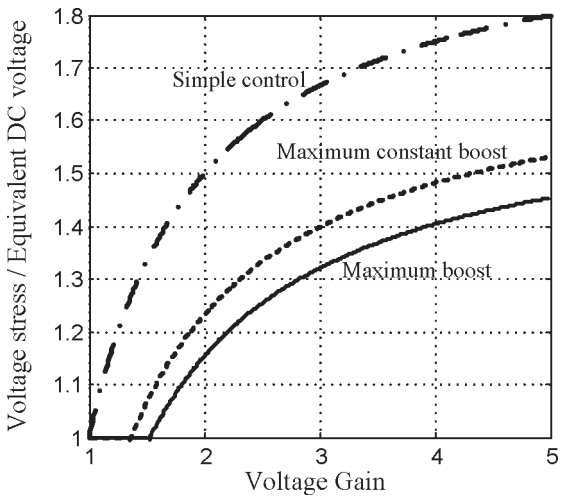

Fig. 9. Voltage-stress comparison of different control methods.

voltage is defined as the minimum dc voltage needed for the traditional voltage-source inverter to produce an output voltage $\hat{V}_{\rm o}$. Obviously, the equivalent dc voltage should be $GV_{\rm dc}$. The ratio of the voltage stress to the equivalent dc voltage represents the cost that the Z-source inverter has to pay to achieve voltage boost.

The voltage stress across the devices $V_{\rm S}$ can be expressed as

$$V_{\rm S} = BV_{\rm dc}. \tag{18}$$

The ratios of the voltage stress to the equivalent dc voltage $V_{\rm S}/(GV_{\rm dc})$ for the simple control, maximum boost control, and maximum constant boost control, respectively, proposed in [1] and [2], and this paper, are summarized as follows:

$$\frac{V_{\rm S}}{GV_{\rm dc}} = \frac{BV_{\rm dc}}{GV_{\rm dc}} = 2 - \frac{1}{G} \text{ for simple control} \tag{19}$$

$$\frac{V_{\rm S}}{GV_{\rm dc}} = \frac{BV_{\rm dc}}{GV_{\rm dc}} = \frac{3\sqrt{3}}{\pi} - \frac{1}{G} \text{ for maximum boost} \tag{20}$$

$$\frac{V_{\rm S}}{GV_{\rm dc}} = \frac{BV_{\rm dc}}{GV_{\rm dc}} = \sqrt{3} - \frac{1}{G} \text{ for maximum constant boost.} \tag{21}$$

Fig. 9 shows the voltage-stress ratios. As can be seen from Fig. 9, the proposed method has a much lower voltage stress across the devices than the simple control, while having a slightly higher voltage stress than the maximum control method. The ideal voltage-stress ratio is one. The proposed method in this paper is highly desirable for applications requiring a voltage gain of two to three. As we can see from the curves, only an extra 30% voltage stress is needed to achieve a voltage gain of 2.5. More importantly, the proposed control method requires the minimum inductance and capacitance because the inductor current and capacitor voltage contain no low-frequency ripples associated with the output voltage, thus reducing the cost, volume, and weight of the Z-source network.

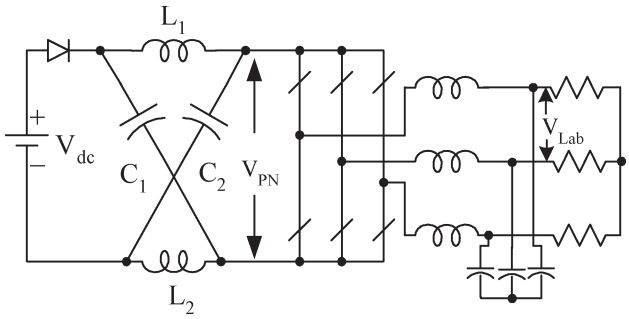

Fig. 10. Simulation and experimental configuration.

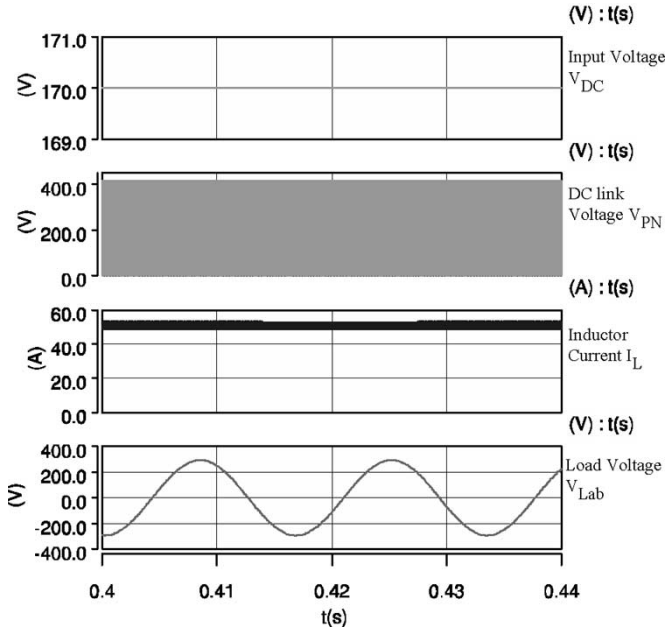

Fig. 11. Simulation results with $M = 0.812$.

V. Simulation and Experimental Results

To verify the proposed control strategies, simulations and experiments were conducted with the configuration shown in Fig. 10 and the following parameters: $L_1 = L_2 = 1$ mH (60-Hz inductor), $C_1 = C_2 = 1300$ μF; switching frequency $=$ 10 kHz; output-filter cutoff frequency $= 1$ kHz, load resistance $= 5$ Ω/phase. The simulation results with the modulation index $M = 0.812$ without third-harmonic injection and $M = 1.1$ with third-harmonic injection are shown in Figs. 11 and 12, respectively, where the input voltages are 170 and 250 V, respectively. Table I lists the theoretical voltage stress and output line-to-line rms voltage based on the previous analysis.

The simulation results in Figs. 11 and 12 are consistent with the theoretical analysis, which verifies the previous analysis and the control concept.

The experimental results with the same operating conditions are shown in Figs. 13 and 14, respectively, which agree well with the analysis and simulation results. For a traditional inverter, to get the output voltage of 208 $V_{\rm rms}$ with modulation

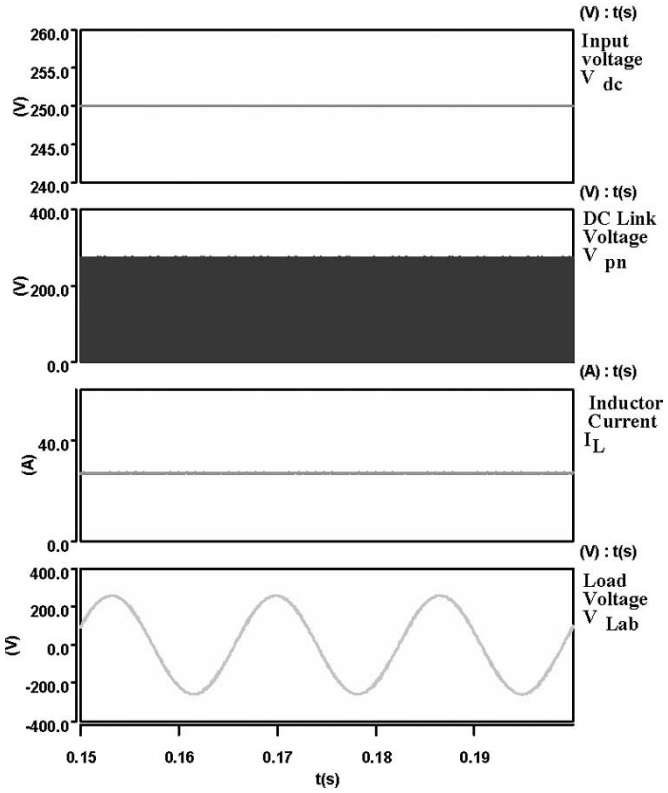

Fig. 12. Simulation results with $M = 1.1$.

TABLE I
THEORETICAL VOLTAGE STRESS AND OUTPUT VOLTAGE UNDER DIFFERENT CONDITIONS

Operating condition	Voltage stress (V)	Output voltage $V_{L\text{-}L}$ (V)
$M = 0.812$, $V_{dc} = 170$V	418	208
$M = 1.1$, $V_{dc} = 250$ V	276	186

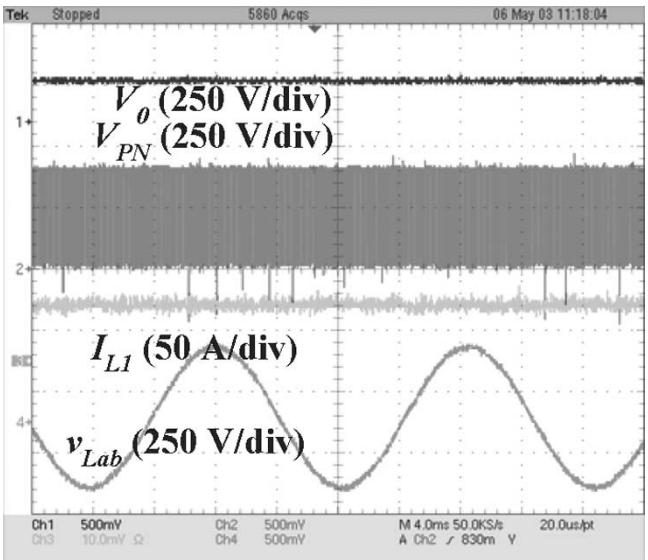

Fig. 13. Experimental results with $V_{\rm dc} = 170$ V and $M = 0.812$.

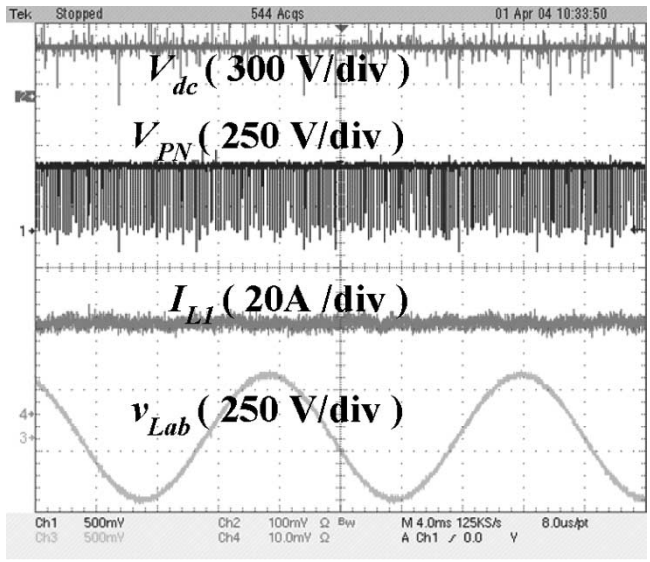

Fig. 14. Experimental results with $V_{\rm dc} = 250$ V and $M = 1.1$.

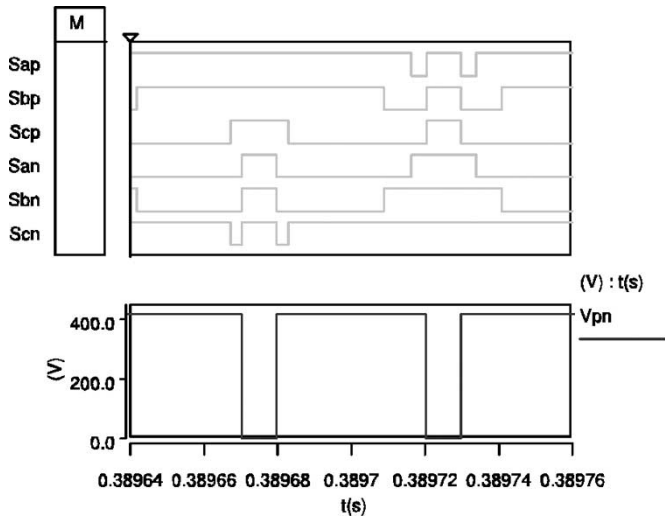

Fig. 15. Detailed simulation result of the PN voltage.

index of one, 340 V dc is required. With boost, the Z-source inverter can produce 208 $V_{\rm rms}$ with only half of the dc link voltage, 170 V. At the same time, the voltage stress across the devices is 418 V, which is allowable for the 600-V devices used in the experimental setup.

Figs. 15 and 16 show the simulation and experimental results of detailed $V_{\rm pn}$. The Z-source inverter's PN voltage ($V_{\rm i}$ in Fig. 1) is no longer a constant dc unlike the traditional voltage-source inverter. It can be clearly seen from the figures that the PN voltage becomes zero when all the six switches are turned on to produce a shoot-through state and a constant level of $(2V_{\rm Cap} - V_{\rm dc})$ during active states. Also, during the shoot-through period, the capacitor is charging the inductor, which is verified by Fig. 16, where we can see that the inductor current increases during the shoot-through state.

Also, from the simulation and experimental results, it is evident that there are no low-frequency (6ω) ripples in the inductor current, which was clearly observed in the maximum

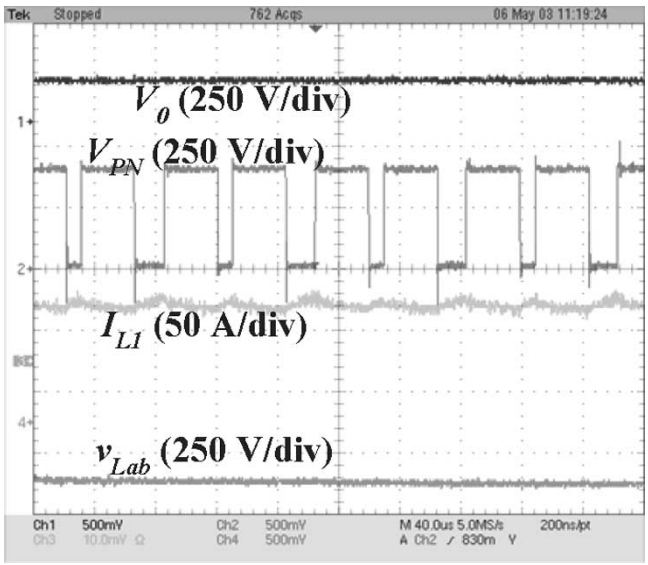

Fig. 16. Detailed experimental results of the PN voltage.

boost control proposed in [2]. The proposed maximum constant boost control only has switching-frequency ripples in the inductor current. The switching-frequency current ripple can be estimated by the current increase during the shoot-through state. For a given modulation index M, the longest shoot-through period is

$$T_0 = \left(1 - \frac{\sqrt{3}}{2}M - \left(\frac{1-M}{2}\right)\right)T_{\rm S} = \frac{1+(1-\sqrt{3})M}{2}T_{\rm S} \tag{22}$$

where $T_{\rm S}$ is the switching cycle. The maximum switching-frequency current ripple $I_{\rm r}$ is

$$I_{\rm r} = \frac{V_{\rm Cap}}{L}\frac{1+(1-\sqrt{3})M}{2}T_{\rm S} = \frac{\frac{\sqrt{3}}{2}MV_{\rm dc}}{\sqrt{3}M-1}\frac{1+(1-\sqrt{3})M}{2L}T_{\rm S} \tag{23}$$

where $V_{\rm Cap}$ is the voltage across the capacitor of the Z-source network. From (23), with the same input voltage, the current ripple increases with the decrease of the modulation index.

To verify that the control method does not introduce any extra harmonic contents compared to the traditional voltage-source inverter with the same modulation index and same output voltage, a simulation was conducted. Fig. 17 shows the simulation results of harmonic contents of output line-to-line voltage after the filter. The simulation condition of the case with shoot through is $M = 0.812$ and $V_{\rm dc} = 170$ V. To make the output voltage the same, the input voltage of 418 V is used for the case of the traditional PWM without shoot through at a modulation index of 0.812. From the simulation results, the harmonic contents of the two cases are almost exactly the same, which means that the shoot through does not introduce any harmonic to the output.

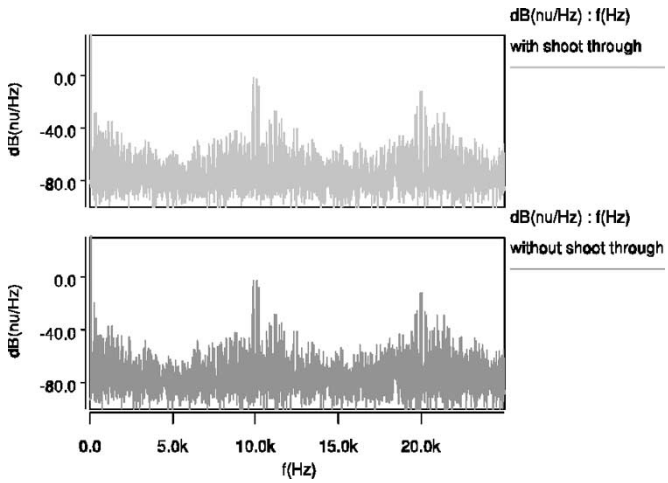

Fig.17. Simulation results of the harmonic contents with and without shoot through.

TABLE II
THEORETICAL VOLTAGE RELATIONSHIP USING SIMPLE CONTROL

Operating condition	Voltage stress (V)	Output voltage $V_{L\text{-}L}$ (V)
$M = 0.812$, $V_{dc} = 260$V	418	208

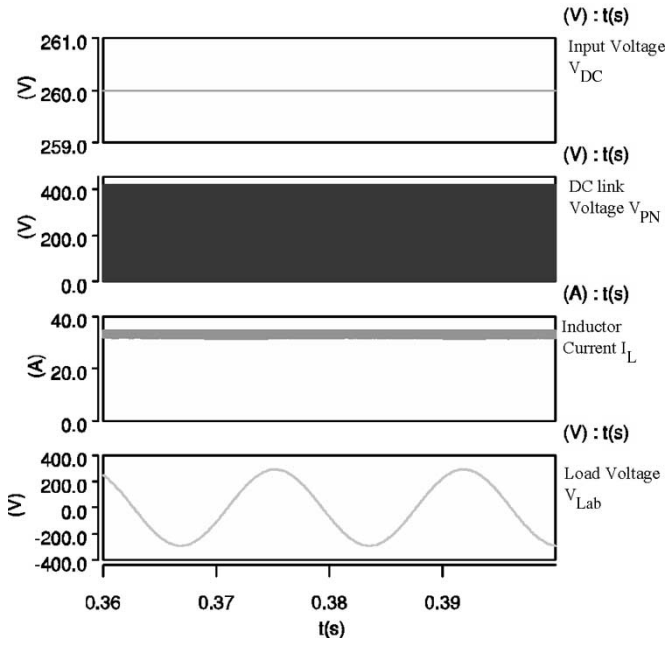

Fig. 18. Simulation results of simple control.

To show the effectiveness of the proposed control method, a comparison with the simple control in [1] is conducted. Using the simple control method with modulation index of 0.812, in order to achieve 208-$V_{\rm rms}$ output voltage, the requested input voltage and resulting voltage stress is shown in Table II.

Simulation and experimental results are obtained with the same setup as shown in Figs. 18 and 19, respectively. From these results, by using the simple control, the input voltage

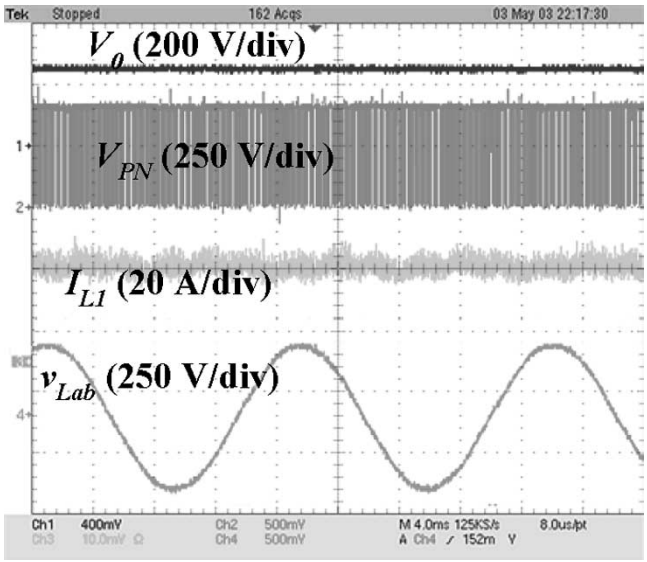

Fig. 19. Experimental results of simple control.

has to be as high as 260 V to achieve the same output voltage versus 170-V input voltage by using the maximum constant boost control while keeping the same voltage stress. In other words, with the same input voltage and the same required output voltage, the maximum constant boost control can achieve much lower voltage stress across the devices than the simple control.

VI. Conclusion

Two control methods to obtain the maximum voltage gain with constant boost have been presented. They achieve maximum voltage boost without introducing any output-frequency-associated 6ω ripples. The relationship of the voltage gain and the modulation index was analyzed in detail. Different control methods have been compared. By using the proposed method, the inverter can achieve the minimum passive-component requirements. Although the presented method will increase the voltage stress across the devices by a small amount compared to the maximum boost method in [2], this method is very suitable for minimizing the Z-source network, especially in low-frequency or variable-speed-drive applications. The control methods have been verified by simulation and experiments.

References

[1] F. Z. Peng, "Z-source inverter," *IEEE Trans. Ind. Appl.*, vol. 39, no. 2, pp. 504–510, Mar./Apr. 2003.
[2] F. Z. Peng, M. Shen, and Z. Qian, "Maximum boost control of the Z-source inverter," *IEEE Trans. Power Electron.*, vol. 20, no. 4, pp. 833–838, Jul./Aug. 2005.
[3] D. A. Grant and J. A. Houldsworth, "PWM ac motor drive employing ultrasonic carrier," in *Proc. IEE Conf. PE-VSD*, London, U.K., 1984 pp. 234–240.
[4] B. K. Bose, *Power Electronics and Variable Frequency Drives*. Upper Saddle River, NJ: Prentice-Hall, 2002.
[5] P. T. Krein, *Elements of Power Electronics*. London, U.K.: Oxford Univ. Press, 1998.
[6] W. Leonard, *Control of Electric Drives*. New York: Springer-Verlag, 1985.
[7] P. C. Loh, D. M. Vilathgamuwa, Y. S. Lai, G. T. Chua, and Y. Li, "Pulse-width modulation of Z-source inverters," in *Conf. Rec. IEEE-IAS Annu. Meeting*, Seattle, WA, 2004, pp. 148–155.

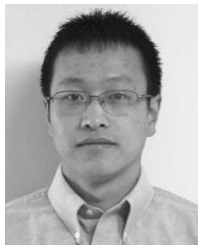

Miaosen Shen (S'04) received the B.S. and M.S. degrees in electrical engineering from Zhejiang University, Hangzhou, China, in 2000 and 2003, respectively. He is currently working toward the Ph.D. degree in electrical engineering at Michigan State University, East Lansing.

His research interests include motor drives, power-factor correction technique, and electronic ballast.

Jin Wang (S'01–M'05) received the B.S. degree from Xi'an Jiatong University, China, in 1998, the M.S. degree from Wuhan University, China, in 2001, and the Ph.D. degree from Michigan State University, East Lansing, in 2005, all in electrical engineering.

He joined Ford Motor Company, Dearborn, MI, in 2005. He is currently a Core Engineer for power electronics systems in Ford's hybrid vehicles. His research interests include hybrid electric vehicles (HEVs)/fuel cell vehicles (FCVs), multilevel converters, dc–dc converters, flexible ac transmission systems (FACTs) devices, and DSP-based control systems.

Alan Joseph received the B.S.E.E. degree from Oakland University, Rochester, MI, in 1998, and the M.S. degree in electrical engineering from Michigan State University, East Lansing, in 2002.

He is with the Department of Electrical and Computer Engineering, Michigan State University, where he conducts research in the areas of multilevel converters, power conversion for alternative energy sources, and variable-frequency drives.

Fang Zheng Peng (M'92–SM'96–F'05) received the B.S. degree from Wuhan University, China, in 1983, and the M.S. and Ph.D. degrees from Nagaoka University of Technology, Japan, in 1987 and 1990, respectively, all in electrical engineering.

He was with Toyo Electric Manufacturing Company, Ltd., Japan, from 1990 to 1992, as a Research Scientist, and was engaged in research and development of active power filters, flexible ac transmission systems (FACTS) applications and motor drives. From 1992 to 1994, he was with Tokyo Institute of Technology as a Research Assistant Professor, where he initiated a multilevel inverter program for FACTS applications and a speed-sensorless vector control project. From 1994 to 2000, he was with Oak Ridge National Laboratory (ORNL), as a Research Assistant Professor at the University of Tennessee, Knoxville, from 1994 to 1997, and was a Staff Member, Lead (Principal) Scientist of the Power Electronics and Electric Machinery Research Center at ORNL from 1997 to 2000. Since 2000, he has been with Michigan State University, East Lansing, as an Associate Professor in the Department of Electrical and Computer Engineering. He is the holder of over ten patents.

Dr. Peng has received many awards, including the 1996 First-Prize Paper Award and the 1995 Second-Prize Paper Award of the Industrial Power Converter Committee at the IEEE/Industry Applications Society Annual Meeting; the 1996 Advanced Technology Award of the Inventors Clubs of America, Inc., the International Hall of Fame; the 1991 First-Prize Paper Award from the IEEE Transactions on Industry Applications; and the 1990 Best Paper Award from the *Transactions of the Institute of Electrical Engineers of Japan*; and the Promotion Award of the Electrical Academy. He was the Chair of the Technical Committee for Rectifiers and Inverters of the IEEE Power Electronics Society from 2001 to 2005 and was an Associate Editor for IEEE Transactions on Power Electronics from 1997 to 2001 and has been an Associate Editor again since 2005.

Leon M. Tolbert (S'88–M'91–SM'98) received the B.E.E., M.S., and Ph.D. degrees in electrical engineering from the Georgia Institute of Technology, Atlanta, in 1989, 1991, and 1999, respectively.

Since 1991, he has worked on several electrical distribution projects at the three U.S. Department of Energy plants in Oak Ridge, TN. In 1999, he joined the Department of Electrical and Computer Engineering, University of Tennessee, Knoxville, where he is presently an Associate Professor. He is an Adjunct Participant at the Oak Ridge National Laboratory (ORNL) Power Electronics and Electric Machinery Research Center. He does research in the areas of electric power conversion for distributed energy sources, reactive power compensation, multilevel converters, hybrid electric vehicles, and application of SiC power electronics.

Dr. Tolbert is a Registered Professional Engineer in the State of Tennessee. He is the Chair of the Educational Activities Committee of the IEEE Power Electronics Society and Chair of the Special Activities, Industrial Power Converter Committee, IEEE Industry Applications Society. He is the recipient of a National Science Foundation CAREER Award and the 2001 IEEE Industry Applications Society Outstanding Young Member Award.

Donald J. Adams (M'95) received the B.S. degree from the University of Mississippi, Oxford, in 1973, and the M.S. degree from the University of Tennessee, Knoxville, in 1977, both in mechanical engineering.

He is the Director of the Power Electronics and Electric Machinery Research Center at Oak Ridge National Laboratory (ORNL), Knoxville, where he has been employed for 29 years. His research interests include advanced inverters and adjustable-speed drives, power transmission and distribution research and development, electric machines, and power quality, efficiency, and power measurements. He is the holder of seven patents with two pending, and has authored numerous publications.

Mr. Adams is a Registered Professional Engineer in the State of Tennessee and is on the Governing Board of the NSF Center for Power Electronics Systems, which consists of five universities and over 80 industrial partners.